P1.58 UPSCALING MICROPHYSICAL PROCESS RATES TO THE GRID BOX SIZE

Vincent E. Larson,* and Brian M. Griffin
Dept. of Mathematical Sciences, University of Wisconsin — Milwaukee, Milwaukee, WI

1. ABSTRACT

Any local microphysics formula that accurately computes microphysical processes at a point in space will still yield inaccurate results if it is driven by inaccurate distributions of moisture and temperature. Inaccuracy occurs when microphysical processes are non-linear, and the variability in moisture and temperature within a grid box is large.

To avoid this inaccuracy, local microphysical formulas may be upscaled to an extensive grid box. Spatial variability within a grid box may be represented by a probability density function (PDF). Then the upscaling may be done by analytically integrating the local microphysical formula over the PDF. In this paper, we analytically upscale the local microphysical formulas of Khairoutdinov and Kogan, which collectively constitute a double-moment scheme for drizzle in marine stratocumulus. Then we implement the upscaled formulas interactively in a single-column model and test the model for a drizzling marine stratocumulus case, namely research flight two (RF02) of the DYCOMS-II field experiment.

Compared to the local microphysics solution, the upscaled microphysics exhibits increased autoconversion of cloud droplets to raindrops and increased accretion of cloud droplets onto raindrops (i.e. increased collection). The combined result is a significant increase in rainwater at the ocean surface, in closer agreement to a benchmark large-eddy simulation.

This conference paper provides a shortened version of Larson and Griffin (2010) and Griffin and Larson (2010). Please refer there for more details.

2. INTRODUCTION

Microphysical processes are often local. Consider, for instance, autoconversion, the process whereby cloud droplets grow to drizzle-drop size. The autoconversion rate at a point in space depends on the population of cloud droplets in the immediate vicinity, not on cloud droplets at distant locations.

However, large-scale atmospheric numerical models of atmospheric flows that compute such microphysical processes typically discretize the domain into large grid boxes and compute fields, e.g. moisture and temperature, only at the grid box scale or larger. Such models require not local microphysical rates, but rather average rates over a grid box that can be used to increment the grid-box-scale moisture and temperature fields.

When we desire a grid-box-average rate, substituting a local microphysical rate is often inaccurate. This is especially true when the microphysical processes are both nonlinear and small in scale.

The non-linearity implies that, for a process rate represented by a nonlinear function f that depends on variable x, usually

$$\langle f(x) \rangle \neq f(\langle x \rangle), \tag{1}$$

where the angled brackets denote a grid-box average (Pincus and Klein 2000). In other words, the grid box average (the left-hand side) does not equal the result of feeding the average of x into the local formula f (the right-hand side), except by coincidence. For example, the grid-box-average cloud water is insufficient information to predict grid-box-average autoconversion rate. One reason is that autoconversion occurs disproportionately in the part of the grid box with more cloud water.

The small-scale nature of such processes allows variability to occur on the subgrid scale. When the subgrid variability is large, the microphysical rates need to be averaged in a way that accounts for this variability. Stated differently, local microphysical formulas, even if perfectly accurate, need to be "upscaled" to the grid box scale.

To do so, a model may estimate, for variables like x, the probability density function (PDF) of spatial variability within a grid box, $P(x)$. Then the model may integrate over the PDF to produce a grid-box average of the microphysical process rate:

$$\langle f(x) \rangle = \int f(x) P(x) dx. \tag{2}$$

In many cases, the PDF provides sufficient information to account for subgrid variability. Given the within-grid-box PDF, a model "knows" how much cloud water is present in the moistest part of a cloudy grid box and therefore "knows" how to weight an autoconversion formula in order to account for the moistest part.

If the PDF can be accurately predicted, then, in many cases, the problem of parameterizing subgrid variability reduces to the problem of quadrature, namely, the integration of Equation (2). The integral can be evaluated via Monte Carlo integration (Pincus et al. 2003; Räisänen et al. 2004; Larson 2007). That is, sample points can be drawn from the PDF, $P(x)$, and fed into the microphysical formula $f(x)$. The resulting points can be averaged to yield an estimate of $\langle f(x) \rangle$. This technique is flexible and is applicable when $f(x)$

*Corresponding author address: Vincent E. Larson, Department of Mathematical Sciences, University of Wisconsin – Milwaukee, P. O. Box 413, Milwaukee, WI 53201-0413, vlarson at uwm dot edu, http://www.uwm.edu/∼vlarson .

is a complex numerical subroutine. However, the technique also introduces statistical noise into the averages due to the necessarily limited sample size (Räisänen and Barker 2004; Räisänen et al. 2005; Larson et al. 2005; Pincus et al. 2006).

Rather than Monte Carlo integration, this paper instead integrates Equation (2) analytically. This yields exact integrals, and in particular avoids the noise associated with Monte Carlo integration. Analytic integration is possible only because we use microphysical formulas $f(x)$ and PDFs $P(x)$ that are simple. Specifically, the microphysical formulas are those of Khairoutdinov and Kogan (2000) (hereafter denoted KK) for drizzling marine stratocumulus clouds. KK parameterize all microphysical sources and sinks in terms of power laws, which greatly simplifies the mathematics. Furthermore, our chosen PDF has a simple functional form. It is a mixture of two multivariate normals, in other words, a sum of two joint Gaussians. (For the precipitation variables, the normal mixture form is transformed from a lognormal form.) Each univariate marginal PDF is a normal mixture. (A univariate marginal PDF is the single-variable PDF that remains when all other variates of the full multivariate PDF are integrated over the entire domain.) This combination of simple functional forms for $f(x)$ and $P(x)$ yields analytically tractable integrals.

This analytic approach was outlined and tested by Larson and Griffin (2006). Further results using this method were presented in Wyant et al. (2007). A related analytic approach has been used by Cheng and Xu (2009) for a single-moment microphysics scheme and a normal mixture PDF for rain.

In order to assess the effects of upscaling, we perform two SCM simulations. The two SCMs are identical, except that one uses local KK microphysics and the other upscales the same local microphysics. The two SCM simulations are then compared to a three-dimensional large-eddy simulation (LES). The LES model simulates the RF02 case using the local KK microphysics. Because the LES model uses an identical case configuration and microphysics as the SCM, the LES serves as a benchmark against which the SCM's representation of microphysics can be measured. We note that this paper does not assess the accuracy of the local KK microphysics; rather it is an assessment of the SCM's ability to account for subgrid variability and thereby accurately drive the local microphysical processes.

The remainder of this paper is organized as follows. Section 3. provides an overview of the local KK prognostic equations. Section 4. presents the functional form of the subgrid PDF. Section 5. compares results from models with upscaled and local microphysics. Section 6. summarizes our results.

3. PROGNOSTIC EQUATIONS FOR DRIZZLE

The KK formulas parameterize drizzle in marine stratocumulus clouds. The KK scheme is double moment in both rain water and cloud water. (This paper will use the word "rain" synonymously with "drizzle" although the KK scheme is designed for small raindrops, that is, drizzle drops.) That is, the KK scheme prognoses both number concentrations and mixing ratios for both rain and cloud water. In our simulations, we prognose number concentration and mixing ratio of rain, but we diagnose cloud water mixing ratio, and we prescribe the number concentration of cloud droplets.

The prognostic equations that we use are based on those of Khairoutdinov and Kogan (2000). We use prognostic equations for grid-box-averaged rain water mixing ratio, r_r (Khairoutdinov and Kogan 2000, Eq. 8):

$$\begin{aligned}\frac{\partial \langle r_r \rangle}{\partial t} = & - \langle w \rangle \frac{\partial \langle r_r \rangle}{\partial z} + \frac{\partial \langle V_{r_r} \rangle \langle r_r \rangle}{\partial z} \\ & + \left\langle \left(\frac{\partial r_r}{\partial t} \right)_{\text{evap}} \right\rangle + \left\langle \left(\frac{\partial r_r}{\partial t} \right)_{\text{auto}} \right\rangle \\ & + \left\langle \left(\frac{\partial r_r}{\partial t} \right)_{\text{accr}} \right\rangle + \frac{\partial}{\partial z} \langle K \rangle \frac{\partial \langle r_r \rangle}{\partial z},\end{aligned} \tag{3}$$

and rain drop concentration per mass of air, N_r

$$\begin{aligned}\frac{\partial \langle N_r \rangle}{\partial t} = & - \langle w \rangle \frac{\partial \langle N_r \rangle}{\partial z} + \frac{\partial \langle V_{N_r} \rangle \langle N_r \rangle}{\partial z} \\ & + \left\langle \left(\frac{\partial N_r}{\partial t} \right)_{\text{evap}} \right\rangle + \left\langle \left(\frac{\partial N_r}{\partial t} \right)_{\text{auto}} \right\rangle \\ & + \frac{\partial}{\partial z} \langle K \rangle \frac{\partial \langle N_r \rangle}{\partial z},\end{aligned} \tag{4}$$

where w is the vertical wind component in $\mathrm{m\ s^{-1}}$, V_{r_r} and V_{N_r} are the sedimentation velocities (defined positive downward) in $\mathrm{m\ s^{-1}}$ of r_r and N_r, respectively, and K is the eddy diffusion coefficient in $\mathrm{m^2\ s^{-1}}$. The subscript evap denotes condensation/evaporation; auto denotes autoconversion, and accr denotes accretion (or collection) of cloud droplets by rain drops.

These equations are supplemented by prognostic equations for total moisture, heat content, and various higher-order moments such as turbulence-related quantities.

4. THE PDF FUNCTIONAL FORM

The subgrid-scale variability in all relevant fields is represented by a single, multi-variate PDF. The PDF that we use is predicted by the Cloud Layers Unified By Binormals (CLUBB) SCM (Golaz et al. 2002a,b; Larson and Golaz 2005). CLUBB assumes that the PDF is a weighted mixture of two multi-variate normal/lognormal distributions. In Golaz et al. (2002a), the PDF, $P(w, \theta_l, r_t)$, was a function of only liquid water potential temperature, θ_l, total water mixing ratio, r_t, and vertical velocity, w. Here, the PDF is extended to include r_r, N_r, and cloud droplet concentration per mass of air, N_c. It can be written $P(w, \theta_l, r_t, r_r, N_r, N_c)$.

The marginal distribution of r_c is diagnosed by truncating the distribution of the extended liquid water, s, at

saturation and adding a delta function at $r_c = 0$ in order to represent clear air. The marginal distributions of r_r, N_r, and N_c are all assumed to be single lognormal distributions. A lognormal shape is suitable for hydrometeor species because it tends to an unskewed shape when its mean is large and a positively skewed shape when its mean is small. Furthermore, a lognormal distribution is positive definite. This property is unimportant for variables such as *total* water mixing ratio (vapor plus liquid), which are non-negative but whose left tail falls off well above zero mixing ratio. However, variables such as *drizzle* mixing ratio often cluster near zero but can never be negative. For such variables, it is important that the PDF allow strong postive skewness and yet ensure that negative values never occur. Additionally, a single lognormal distribution has the virtue of simplicity. The form of the PDF for a single variable, x, that is distributed lognormally is:

$$P(x) = \left[(2\pi)^{1/2}\sigma x\right]^{-1} \exp\left[\frac{-(\ln x - \mu)^2}{2\sigma^2}\right], \quad (5)$$

where μ and σ^2 are the mean and the variance, respectfully, of $\ln x$, which is normally distributed.

In order to compute grid box averages that account for subgrid variability, we need to integrate local microphysical formulas over the PDF, as in Equation (2). To do so, it proves mathematically convenient to transform lognormal PDFs to normal ones.

Once the lognormally-distributed variables (r_r, N_r, and N_c) have been transformed into normally-distributed variables, the PDF may be written as a weighted mixture of two 6-variate normal distributions:

$$\begin{aligned} &P(w, \theta_l, r_t, r_{rn}, N_{rn}, N_{cn}) \\ &= (a)\, P_{(1)}(w, \theta_l, r_t, r_{rn}, N_{rn}, N_{cn}) \\ &\quad + (1-a)\, P_{(2)}(w, \theta_l, r_t, r_{rn}, N_{rn}, N_{cn}), \end{aligned} \quad (6)$$

where a is the mixture fraction, which is the relative weight of the first normal distribution, and where:

$$\begin{aligned} &P_{(i)}(w, \theta_l, r_t, r_{rn}, N_{rn}, N_{cn}) \\ &= \frac{1}{(2\pi)^3 \left|\mathbf{\Sigma}_{(i)}\right|^{1/2}} \\ &\quad \times \exp\left\{-\frac{1}{2}\left(\mathbf{x} - \mu_{(i)}\right)^T \mathbf{\Sigma}_{(i)}^{-1}\left(\mathbf{x} - \mu_{(i)}\right)\right\}. \end{aligned} \quad (7)$$

Here $\mathbf{x} = (w, \theta_l, r_t, r_{rn}, N_{rn}, N_{cn})$ is a column vector of variables, and $\mu_{(i)}$ and $\mathbf{\Sigma}_{(i)}$ denote the mean vector and covariance matrix, respectively, of the ith normal of those variables. An important note is that each subset of $\mathbf{x}$ is distributed according to a multivariate normal. The means and variances of r_{rn}, N_{rn}, and N_{cn} are equal for each normal component. For example, in the case of r_{rn}, $\mu_{r_{rn(1)}} = \mu_{r_{rn(2)}}$ and $\sigma^2_{r_{rn(1)}} = \sigma^2_{r_{rn(2)}}$. Hence, for these variates, the two normal components overlap exactly, thereby reducing to a single normal. When transformed back, these variates are distributed according to a single lognormal.

5. MODEL RESULTS

In this section, we present simulations of the DYCOMS-II RF02 marine Sc case using 3 models: the SCM with upscaled microphysics, the SCM with local microphysics, and the SAM benchmark LES. The LES uses the local KK microphysics, but it includes information on horizontal variability of the microphysical fields because it solves the governing equations on a fine-scale three-dimensional mesh. This allows the LES to drive the local microphysical process rates using the spatially varying values of microphysical fields such as N_c and r_r. The local microphysics contains information about the horizontal variability of r_t, θ_l, and w, but not the microphysical fields such as r_r. The upscaled microphysics represents this microphysical variability but in the approximate form of a PDF whose functional form is assumed. The goal of this section is to assess whether or not the upscaled microphysics matches the rain fields simulated by the LES better than the local microphysics.

5.1 Turbulence, thermodynamic, and cloud fields

Before we turn to the rain fields, we first assess whether or not other important fields produced by the SCM simulations match the LES, such as those related to cloud water. Such fields influence rain production, and if they are not simulated accurately, they can lead to inaccurate prediction of rain mixing ratio even if accurate local or upscaled rain processes are used. (Production of rain is defined to consist of two processes: autoconversion of (small) cloud droplets to (large) raindrops, and accretion (i.e. collection) of cloud droplets onto raindrops.)

The profiles of cloud water, $\langle r_c \rangle$, and cloud fraction are similar for all three models (see Figure 1). Cloud water $\langle r_c \rangle$ has the same peak magnitude for all three models, and all three clouds are overcast with about the same thickness. However, both cloud top and cloud base are located slightly lower in the SCM simulations than in the LES. Presumably, the reason is that the SCM simulations do not entrain as much above-cloud air as the LES.

Not only do all three SCM simulations produce similar profiles of mean cloud water, but they also produce similar profiles of horizontal variance in cloud water mixing ratio, $\left\langle r_c^{'2} \right\rangle$ (see Figure 1). Variability in r_c, in addition to its horizontal average, influences rain because rain production is a nonlinear process.

The similarity of the cloud water fields among the models suggests that the differences in rain water fields discussed below are not related to differences in the cloud water itself but rather to the neglect or inclusion of subgrid variability within the microphysics.

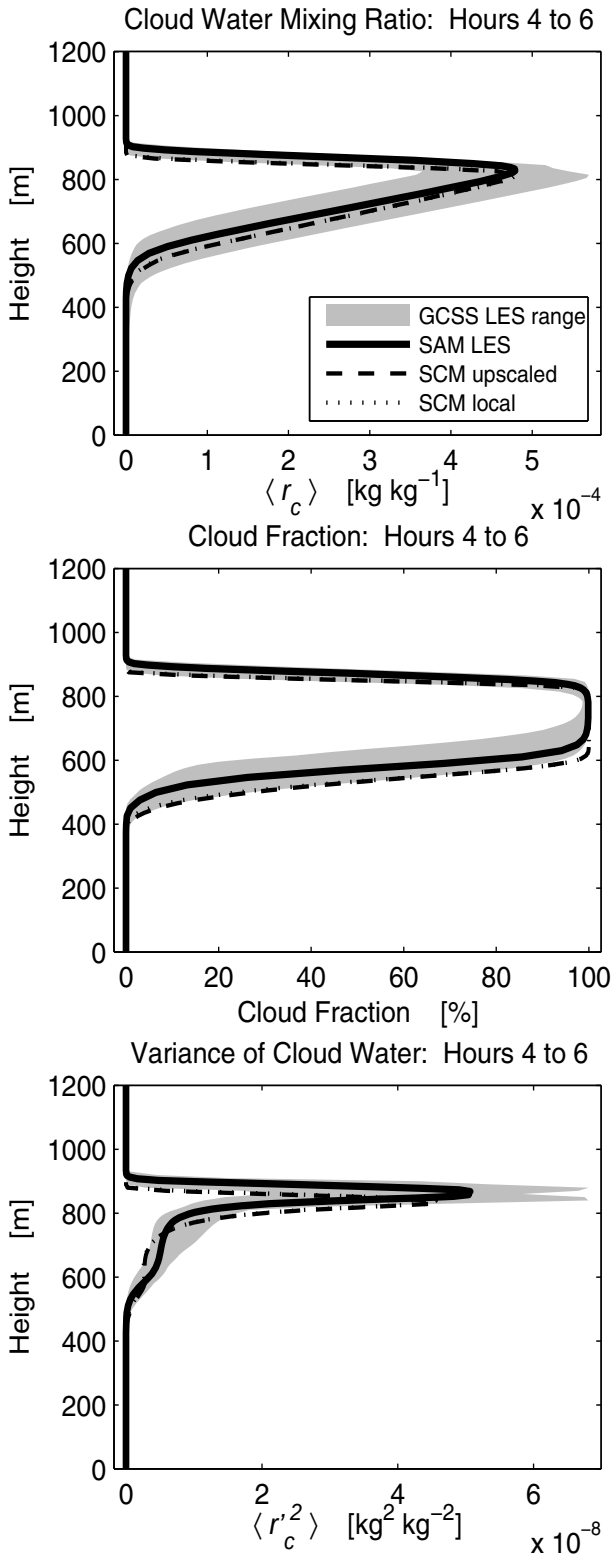

Figure 1: Profiles of $\langle r_c \rangle$ (top), cloud fraction (center), and $\left\langle r_c'^2 \right\rangle$ (bottom) averaged over hours 4 to 6. Shown are profiles from horizontally averaged SAM LES results (thick solid), the SCM with upscaled microphysics (thin dashes) and the SCM with local microphysics (thin dotted). The cloud water profiles are similar among all three simulations. This allows for direct comparison of the rain found in all three simulations because cloud water is an influential factor in rain production.

5.2 Rain

Differences between SAM, the SCM with upscaled microphysics, and the SCM with local microphysics first appear in the rain-related fields. The upscaled microphysics produces more rain at all altitudes than does the local microphysics. For instance, depending on altitude, the upscaled $\langle r_r \rangle$ is a factor of 1.1 to 3.5 times larger than the local $\langle r_r \rangle$. Furthermore, the upscaled raindrop number concentration, $\langle N_r \rangle$, and the precipitation flux are larger at all altitudes than their local counterparts (Figure 2). The upscaled $\langle r_r \rangle$, $\langle N_r \rangle$, and precipitation flux better match the LES near cloud top and especially near the ocean surface (see Figure 2).

Near the ocean surface, the local $\langle r_r \rangle$, $\langle N_r \rangle$, and precipitation flux are all an order of magnitude less than SAM LES. The upscaled SCM still underestimates SAM LES, but at later times lies within the range of the LES that participated in the GCSS intercomparison.

The time series of liquid water path and surface precipitation flux are presented in Figure 3. The liquid water path of all three models is similar, indicating that the microphysics of all three models experience similar environments. Nevertheless, the local microphysics underestimates the surface precipitation flux, whereas the upscaled microphysics mostly lies within the range of LES in the GCSS intercomparison. The fact that LWP is similar among the models but the surface precipitation differs suggests that rain does not strongly deplete liquid water in these simulations. As an aside, we also note that the time evolution of the precipitation fields is smooth, as desired.

6. CONCLUSIONS

This paper upscales a local microphysical scheme for drizzle marine stratocumulus (Khairoutdinov and Kogan 2000) to a larger, grid-box scale. The upscaling is achieved by analytically integrating the Khairoutdinov-Kogan formulas over a multi-variate PDF that represents subgrid variability. The main results are grid-box averaged formulas for drizzle sedimentation velocity, autoconversion rate, accretion rate, and condensation/evaporation rate (Larson and Griffin 2010).

To obtain these formulas, we use PDFs that are assumed mixtures of normal distributions or assumed lognormal distributions, and we use local microphysical formulas that are in the form of power laws. This allows analytic integration in the case of 2- and even 3-variable power laws with positive but arbitrary exponents. The formulas are fairly general. They apply to any power laws. In principle, such power laws could be used to approximate any local process, not merely liquid-phase microphysics, but also ice- or mixed-phase microphysics, or other processes.

Analytic integration is a method of upscaling that offers an alternative to Monte Carlo integration (e.g. Larson et al. 2005). Both methods have strengths and weaknesses. Analytic integration is accurate, but it requires that complex processes, such as microphysics,

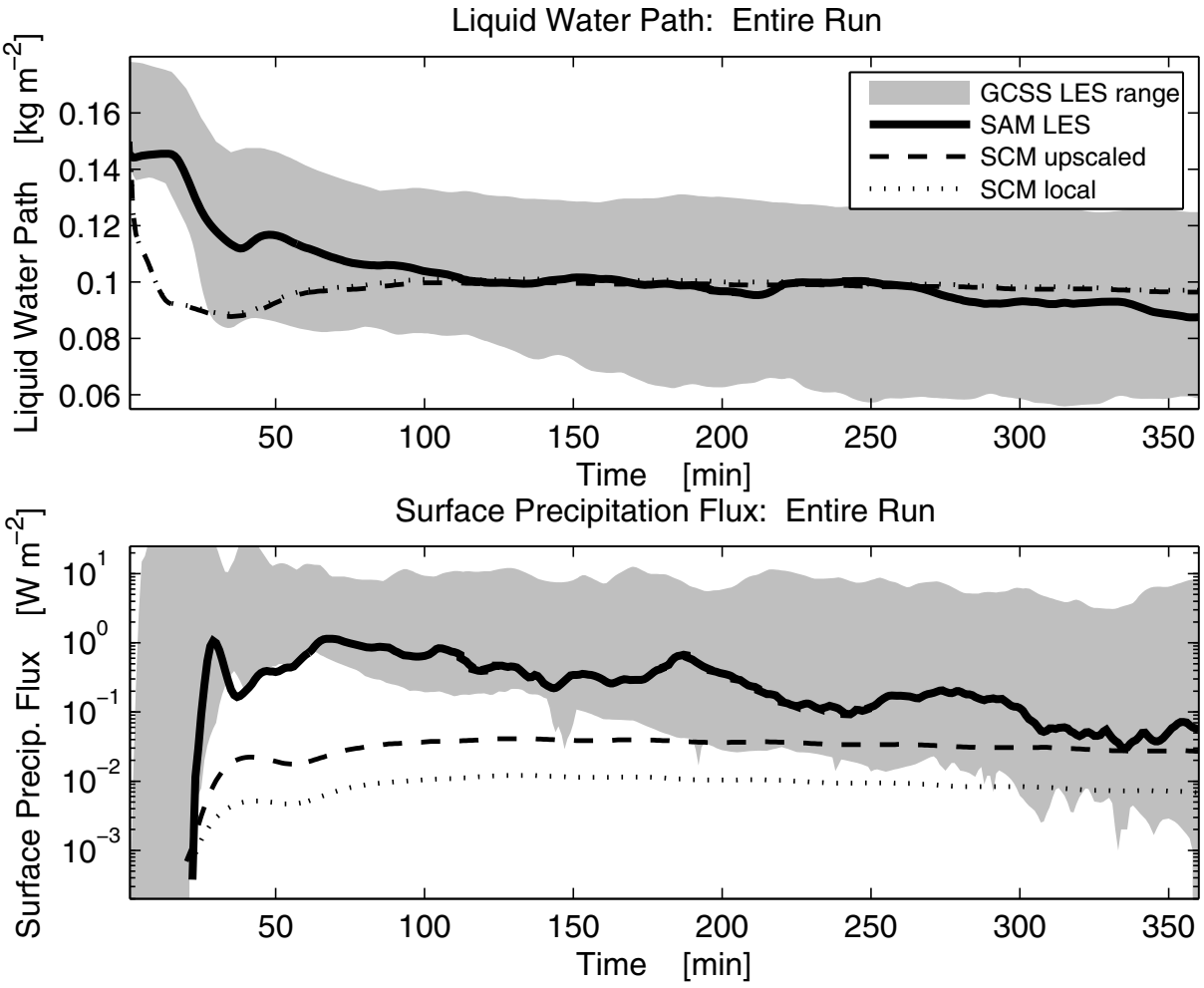

Figure 3: Time series of liquid water path (LWP) (top) and surface precipitation flux (bottom) over the entire course of the simulation. The figure shows results from SAM LES (thick solid lines), the SCM with upscaled microphysics (thin dashed lines), and the SCM with local microphysics (thin dotted lines). All three models produce similar LWP, once again suggesting that the forcing of rain production is similar in all three models. Nevertheless, although both SCM simulations underestimate surface precipitation, the upscaled version produces considerably more than does its local counterpart.

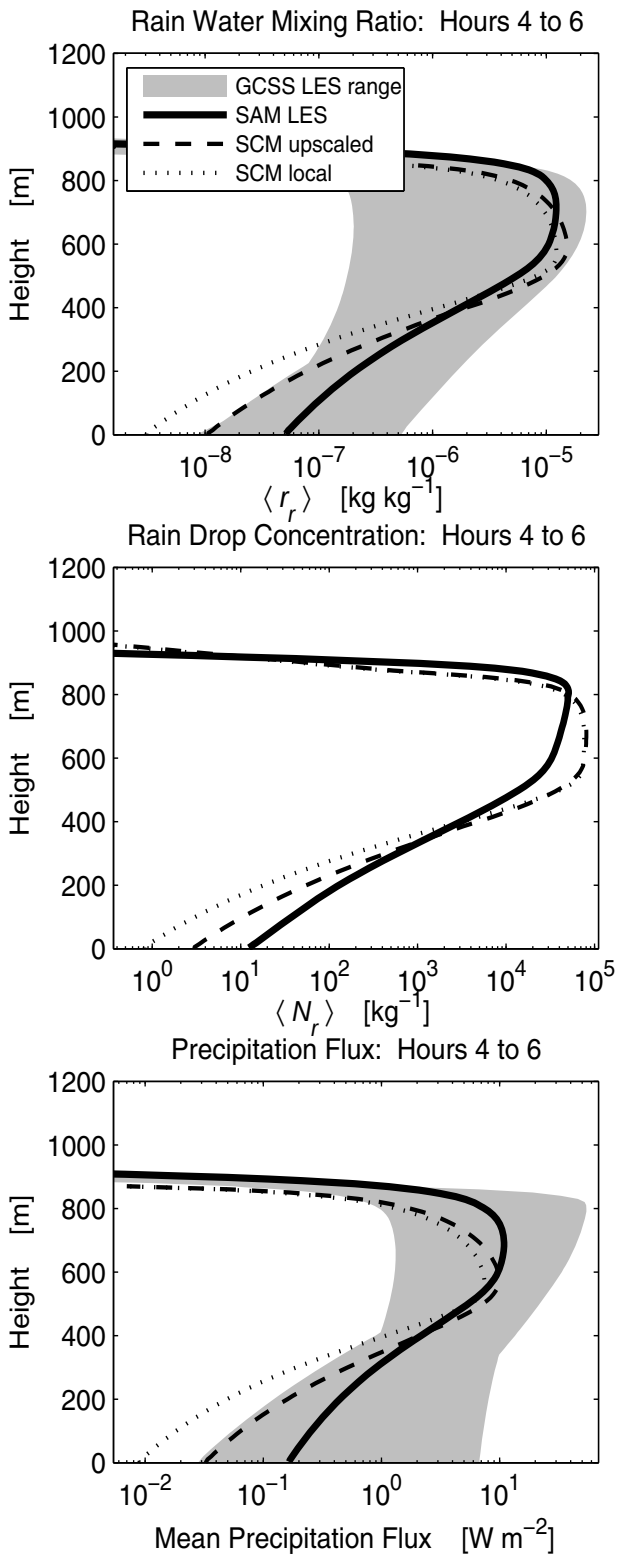

Figure 2: Profiles of $\langle r_r \rangle$ (top), $\langle N_r \rangle$ (center), and precipitation flux (bottom) averaged over hours 4 to 6. The thicker, solid lines represent the results of the horizontally averaged SAM LES; the thin, dashed lines, the SCM with upscaled microphysics; and the thin, dotted lines, the SCM with local microphysics. The upscaled microphysics produces more rain than does the local microphysics. Furthermore, the upscaled microphysics usually agrees more closely with SAM than does the local microphysics.

be represented by simple formulas, such as power laws. Monte Carlo integration introduces sampling noise, but is applicable to a broad range of diagnostic parameterization formulas, including ones in the form of numerical subroutines.

In this paper, we evaluate the analytic upscaling method. To do so, we implement upscaled microphysics into the single-column model (SCM) of Golaz et al. (2002a). Then we simulate a drizzling marine stratocumulus cloud that was observed during Research Flight 2 (RF02) of the DYCOMS-II field experiment (Stevens et al. 2003). We simulate the RF02 case using 1) the SCM with upscaled microphysics; 2) the same SCM except that subgrid variability in clouds does *not* drive microphysics, and subgrid variability is neglected in the hydrometeor fields (but not the thermodynamic or turbulence fields); 3) and a three-dimensional benchmark large-eddy simulation (LES) model. The three simulations are configured identically insofar as possible, thereby allowing direct comparison among them. Furthermore, all three simulations produce similar fields of cloud water mixing ratio (r_c), horizontal variance of r_c, and humidity below cloud. Therefore, the cloud and humidity fields in all three simulations drive the drizzle processes similarly.

The SCM with upscaled microphysics produces nearly four times as much precipitation flux at the ocean surface as does the SCM with local microphysics. The profile of *upscaled* precipitation flux lies mostly within the range simulated by LES models participating in the RF02 GCSS intercomparison, but the *local* precipitation flux does not (Figure 2). Relatedly, upscaling the microphysics increases $\langle r_r \rangle$ by about 20% within cloud and about 75% at the surface. Differences in rain of this magnitude can also arise from changes in the formulation of local microphysical formulas (e.g., Cotton and Anthes 1989). Nevertheless, our results demonstrate that accounting for subgrid variability has a non-negligible effect in the RF02 case.

Why does accounting for subgrid variability increase rain? The upscaled rain is enhanced by increased autoconversion and accretion, which outweighs the diminishment of rain by enhanced evaporation. Within cloud, accounting for subgrid variability increases the autoconversion rate by an average of 20%, increases the accretion rate by an average of 13%, and increases the evaporation rate by an average of 10%.

7. ACKNOWLEDGMENTS

The authors are grateful for financial support provided by Grant 04-062 from the UWM Research Growth Initiative and by Grants ATM-0618818 and ATM-0936186 from the National Science Foundation.

References

Cheng, A. and K.-M. Xu, 2009: A pdf-based microphysics parameterization for simulation of drizzling

boundary layer clouds. *J. Atmos. Sci.*, **66**, 2317–2334.

Cotton, W. R. and R. A. Anthes, 1989: *Storm and Cloud Dynamics*. Academic Press, 884 pp.

Golaz, J.-C., V. E. Larson, and W. R. Cotton, 2002a: A PDF-based model for boundary layer clouds. Part I: Method and model description. *J. Atmos. Sci.*, **59**, 3540–3551.

Golaz, J.-C., V. E. Larson, and W. R. Cotton, 2002b: A PDF-based model for boundary layer clouds. Part II: Model results. *J. Atmos. Sci.*, **59**, 3552–3571.

Griffin, B. M. and V. E. Larson, 2010: Analytic upscaling of local microphysics parameterizations, Part II: Simulations. Submitted to *Quart. J. Royal Met. Soc.*.

Khairoutdinov, M. and Y. Kogan, 2000: A new cloud physics parameterization in a large-eddy simulation model of marine stratocumulus. *Mon. Wea. Rev.*, **128**, 229–243.

Larson, V. E., 2007: From cloud overlap to PDF overlap. *Quart. J. Royal Met. Soc.*, **133**, 1877–1891. doi:10.1002/qj.165.

Larson, V. E. and J.-C. Golaz, 2005: Using probability density functions to derive consistent closure relationships among higher-order moments. *Mon. Wea. Rev.*, **133**, 1023–1042.

Larson, V. E. and B. M. Griffin, 2006: Coupling microphysics parameterizations to cloud parameterizations. Preprints*, 12th Conference on Cloud Physics*, Madison, WI, American Meteorological Society.

Larson, V. E. and B. M. Griffin, 2010: Analytic upscaling of local microphysics parameterizations, Part I: Theory. Submitted to *Quart. J. Royal Met. Soc.*.

Larson, V. E., J.-C. Golaz, H. Jiang, and W. R. Cotton, 2005: Supplying local microphysics parameterizations with information about subgrid variability: Latin hypercube sampling. *J. Atmos. Sci.*, **62**, 4010–4026.

Pincus, R. and S. A. Klein, 2000: Unresolved spatial variability and microphysical process rates in large-scale models. *J. Geophys. Res.*, **105**, 27059–27065.

Pincus, R., H. W. Barker, and J.-J. Morcrette, 2003: A fast, flexible, approximate technique for computing radiative transfer in inhomogeneous cloud fields. *J. Geophys. Res.*, **108**, Art. No. 4376.

Pincus, R., R. Hemler, and S. A. Klein, 2006: Using stochastically-generated subcolumns to represent cloud structure in a large-scale model. *Mon. Wea. Rev.*, **134**, 3644–3656.

Räisänen, P. and H. W. Barker, 2004: Evaluation and optimization of sampling errors for the Monte Carlo Independent Column Approximation. *Quart. J. Roy. Meteor. Soc.*, **130**, 2069–2085.

Räisänen, P., H. W. Barker, M. F. Khairoutdinov, J. Li, and D. A. Randall, 2004: Stochastic generation of subgrid-scale cloudy columns for large-scale models. *Quart. J. Roy. Meteor. Soc.*, **130**, 2047–2067.

Räisänen, P., H. W. Barker, and J. N. S. Cole, 2005: The Monte Carlo Independent Column Approximation's conditional random noise: Impact on simulated climate. *J. Climate*, **18**, 4715–4730. doi:10.1175/JCL13556.1.

Stevens, B., D. H. Lenschow, G. Vali, H. Gerber, A. Bandy, B. Blomquist, J.-L. Brenguier, C. S. Bretherton, F. Burnet, T. Campos, S. Chai, I. Faloona, D. Friesen, S. Haimov, K. Laursen, D. K. Lilly, S. M. Loehrer, S. P. Malinowski, B. Morley, M. D. Petters, D. C. Rogers, L. Russell, V. Savic-Jovcic, J. R. Snider, D. Straub, M. J. Szumowski, H. Takagi, D. C. Thornton, M. Tschudi, C. Twohy, M. Wetzel, and M. C. Van Zanten, 2003: Dynamics and chemistry of marine stratocumulus – DYCOMS-II. *Bull. Amer. Meteor. Soc.*, **84**, 579–593.

Wyant, M. C., C. S. Bretherton, A. Chlond, B. M. Griffin, H. Kitagawa, C.-L. Lappen, V. E. Larson, A. Lock, S. Park, S. R. de Roode, J. Uchida, M. Zhao, and A. S. Ackerman, 2007: A single-column-model intercomparison of a heavily drizzling stratocumulus topped boundary layer. *J. Geophys. Res.*, **112**. doi:10.1029/2007JD008536.